

A Theoretical, Spectroscopic, and Photophysical Study of 2,7-Carbazolenevinylene-Based Conjugated Derivatives

Michel Belletête,[†] Jean-François Morin,[‡] Mario Leclerc,[‡] and Gilles Durocher^{*,†}

Laboratoire de photophysique moléculaire, Département de Chimie, Université de Montréal, C.P. 6128, Succ. Centre-Ville, Montréal, Québec, H3C 3J7, Canada, and Laboratoire des polymères photoactifs et électroactifs, Centre de recherche en sciences et ingénierie des macromolécules (CERSIM), Université Laval, Cité Universitaire, Québec, G1K 7P4, Canada

Received: March 15, 2005; In Final Form: June 13, 2005

A combined theoretical and experimental study of the structure, optical, and photophysical properties of four 2,7-carbazolenevinylene-based derivatives in solution is presented. Geometry optimizations of the ground states of PCP, PCP-CN, TCT, and TCT-CN were carried out using the density functional theory (DFT/B3LYP/6-31G*). It is found that PCP and TCT are nearly planar in their ground electronic states (S_0), whereas the cyano derivatives are more twisted. The nature and the energy of the first singlet–singlet electronic transitions have been obtained from time-dependent density functional theory (TDDFT) calculations performed on the optimized geometries. For all the compounds, excitation to the S_1 state corresponds mainly to the promotion of one electron from the highest-occupied molecular orbital to the lowest-unoccupied molecular orbital, and the $S_1 \leftarrow S_0$ electronic transition is strongly allowed and polarized along the long axis of the molecular frame. The optimization (relaxation) of the first singlet excited electronic state (S_1) has been done using the restricted configuration interaction (singles) (RCIS/6-31G*) approach. It is observed that all four investigated compounds become more planar in their S_1 relaxed excited state. Electronic transition energies from the relaxed excited states have been obtained from TDDFT calculations performed on the S_1 -optimized geometries. The absorption and fluorescence spectra of the carbazolenevinylenes have been recorded in chloroform. A good agreement is obtained between TDDFT vertical transitions energies and the (0,0) absorption and fluorescence bands. The change from phenylene to thiophene rings as well as the incorporation of cyano substituents induce bathochromic shifts in the absorption and fluorescence spectra. From the analysis of the energy of the frontier molecular orbitals, it is believed that thiophene rings and CN substituents induce some charge-transfer character to the first electronic transition, which is responsible for the red shifts observed. Finally, the fluorescence quantum yield and the lifetime of the compounds in chloroform have been obtained. In sharp contrast with many oligothiophenes, it is observed that TCT possesses a high fluorescence quantum yield. On the other hand, the CN-containing derivatives exhibit much lower fluorescence quantum yields, probably due to the combined influence of steric effects and charge-transfer interactions caused by the cyano groups.

1. Introduction

Within the last two decades, conjugated organic oligomers and polymers have reached the role of a major, technologically important class of materials. Conjugated organic polymers have the advantages of low cost, ease of modification of properties by appropriate substitution, and of solvent processability. Major applications include the development of electronic devices such as field-effect transistors,^{1–3} solar cells,^{4,5} and light-emitting diodes (LED).^{6–10} Recently, the synthesis of various well-defined conjugated oligomers and polymers derived from phenylene, pyrrole, thiophene, and fluorene moieties has been achieved. However, the fabrication of novel materials for future electronic devices from conjugated building blocks is still a challenge.

Recently, we have reported the synthesis and characterization of novel well-defined 2,7-carbazole-based oligomers^{11–13} and

polymers.^{14–19} Quantum chemical calculations have also been performed on carbazole-based dyads and triads to gain insight into the nature of the electronic transitions. Good agreement has been found between theoretical and electronic transitions (excitation and emission energies) and experimental spectra (absorption and fluorescence).^{11–13} Luminescent materials spanning the entire visible range have been prepared from these polymers,²⁰ which can be useful as LEDs.^{21,22}

The introduction of a vinylene unit into the polymer backbone is a well-known method to decrease the band gap of aromatic polymers and to fine tune their electrical properties.²³ In particular, poly(*p*-phenylenevinylene) (PPV) and its derivatives have received considerable attention during the last two decades.^{24–25} Moreover, to increase the electron affinity of PPV, CN substituents have been attached either on the double bonds^{26–29} or on the aromatic rings.^{30,31} The introduction of electron-withdrawing cyano groups on the vinylene moieties in a PPV reduces the barrier for electron injection into the polymer and improves the electron-transporting properties.³² Along these lines, Leclerc's research group has reported the

* To whom correspondence should be addressed. Tel.: 514-343-6911. Fax: 514-343-7586. E-mail: gilles.durocher@umontreal.ca.

[†] Université de Montréal.

[‡] Université Laval.

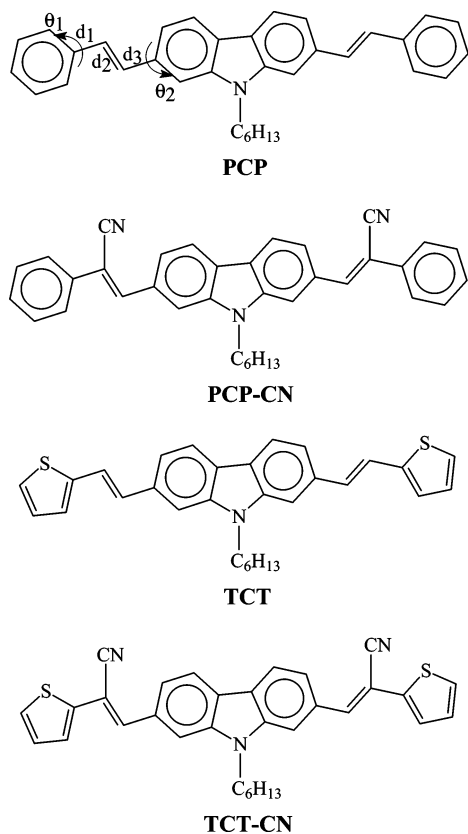


Figure 1. Molecular structure of the 2,7-carbazole-vinylenes.

synthesis and characterization of novel 2,7-carbazolevinylene-based conjugated derivatives and polymers (with and without cyano groups).³³ To learn more about the structure–property relationships in this new class of materials and particularly the role played by the cyano group, we report herein the ground and excited-state properties as well as the optical and photophysical properties of four 2,7-carbazolevinylene-based conjugated compounds, namely, PCP, PCP-CN, TCT, and TCT-CN, which are illustrated in Figure 1. First, a ground S_0 state geometry optimization is performed using the density functional theory (DFT/B3LYP/6-31G*). Next, the energy of the $S_1 \leftarrow S_0$ transitions are computed by time-dependent density functional theory (TDDFT) calculations performed for the ground-state-optimized geometries. Then the S_1 excited states are optimized using the restricted configuration interaction (singles) (RCIS/6-31G*) approach, and the $S_1 \rightarrow S_0$ electronic transitions from the relaxed excited states are obtained from TDDFT calculations using optimized excited states as inputs. Finally, the optical properties and the photophysics of these derivatives have been measured in chloroform. The absorption and fluorescence spectra of the carbazolevinylenes (the ethyl chains are replaced by hexyl groups in the actual compounds) are correlated to the theoretical results. Good agreement is obtained between the computed electronic transitions and the optical data. The photophysical results are discussed in terms of the relative importance of the radiative and nonradiative processes occurring in these materials.

2. Experimental Section

2.1. Computational Methodology. The optimization of the ground-state geometry of the four carbazolevinylenes investigated was performed by DFT.^{34,35} The DFT method, implemented in the Gaussian 03W software,³⁶ was chosen because of its good compromise between computational time and

accuracy. In this work, the DFT calculations were performed using the hybrid Becke3 (exchange)³⁷ and the Lee–Yang–Parr (correlation)³⁸ functionals (B3LYP) in conjunction with a modest 6-31G* split-valence polarized basis set.³⁹ It is well understood that, in general, DFT/B3LYP/6-31G* calculations provide accurate geometries for conjugated derivatives.⁴⁰ The geometry optimization was carried out by changing the atom coordinates until the total energy was minimized. Standard options were used for the self-consistent field (SCF) convergence and threshold limits in the optimization. In all cases, the geometry was fully optimized without any geometrical restrictions, and it was considered to be adequately concluded when the analysis of the vibrational frequencies did not give any imaginary frequency.

The molecular orbital energies and the $S_1 \leftarrow S_0$ electronic transitions were calculated from the optimized geometry of the S_0 state by TDDFT,^{41,42} supplied in Gaussian 03W, with the hybrid B3LYP functional and the 6-31G* basis set. Some studies have indicated that hybrid functionals give better performance for evaluating the transition energies of organic molecules.^{43–45} In particular, Yu et al. have suggested that B3LYP is the optimal functional to use for excited-state calculations on PPV polymers.⁴⁶ Moreover, recently we have compared excited-state properties of ladder oligo(*p*-aniline)s as obtained by TDDFT/B3LYP/6-31G*, which use an atom-centered basis set, with those calculated from a DFT approach based on a plane-wave basis set, with the local density approximation (TDDFT/LDA/PW).⁴⁷ It was observed that the electronic excitations of these derivatives obtained by the two TDDFT calculations are close in energy. This is a clear indication of the robustness of the TDDFT approach, regarding the basis set used in the calculations.

The geometry optimization of the first excited S_1 state was carried out using the ab initio method restricted configuration interaction singles (RCIS)⁴⁸ incorporated in the Gaussian 03W software. The 6-31G* basis set was chosen for all derivatives. TDDFT/B3LYP/6-31G* calculations were used to calculate $S_1 \rightarrow S_0$ electronic excitations from the optimized (relaxed) S_1 state. These calculations were performed over geometries optimized by the RCIS method.

2.2. Materials and Methods. The 2,7-carbazole vinylene compounds, shown in Figure 1, were synthesized and purified following similar procedures than those reported earlier.³³ Chloroform was supplied by A&C American Chemicals Ltd. (spectrograde) and used without any further purification. Prior to use, the solvent was checked for spurious emission in the region of interest and found to be satisfactory.

All experiments were carried out at room temperature. UV–Vis absorption spectra of the derivatives in chloroform were recorded on a Varian Cary 1 Bio UV/Vis spectrophotometer using 1-cm quartz cells and solute concentrations of $(1–3) \times 10^{-5}$ M. The molar extinction coefficients (ϵ) at absorption maxima were obtained from the slope of the absorbance vs the concentration using seven solutions of different concentrations. Fluorescence excitation and emission spectra were recorded on a Fluorolog-2 spectrofluorometer, with correction for instrumental factors by means of a rhodamine B quantum counter and correction files supplied by the manufacturer. Excitation and emission band-passes used were 2.6 and 1.9 nm, respectively. Each solution was excited near the wavelength of the absorption maximum using a 1-cm path length quartz cell. Solution concentrations used were $(1–3) \times 10^{-6}$ M, giving absorbances always less than 0.1 to avoid any inner-filter effects. For all molecules, a study of the concentration (*C*) effect has

TABLE 1: Dihedral Angles and Bond Distances between Subunits of Carbazolenevinylene Derivatives in Their S_0 Ground Electronic State as Calculated by the DFT/B3LYP/6-31G* Method

molecules	dihedral angles (deg)		bond distances (Å)		
	θ_1	θ_2	d_1	d_2	d_3
PCP	4.7	3.8	1.466	1.348	1.463
PCP-CN	28.5	6.1	1.489	1.364	1.457
TCT	1.6	2.9	1.450	1.352	1.461
TCT-CN	23.8	5.8	1.470	1.367	1.455

been done on the fluorescence intensity (I_F), and all measurements have been performed in the linear region of the I_F vs C curve. The corrected fluorescence excitation spectra were found to be equivalent to the respective absorption spectra. Moreover, the fluorescence and excitation spectra were found to be independent of the excitation and emission wavelengths, respectively. Fluorescence quantum yields were measured relative to 9,10-diphenylanthracene in cyclohexane ($\phi_f = 0.90$) as standard.⁴⁹ Fluorescence lifetimes were determined by single-photon counting using a commercially available Edinburgh Instruments, model 299T spectrometer equipped with a hydrogen-filled nanosecond flashlamp and the analysis software supplied by the manufacturer. Details on the instrument have been published elsewhere.⁵⁰ Theoretical equations were fitted to experimental data by means of a nonlinear weighted least-squares routine based on the Marquardt algorithm. The kinetic interpretation of the goodness-of-fit was assessed using plots of weighted residuals, reduced χ^2 values, and Durbin–Watson (DW) parameters.

3. Results and Discussion

3.1. Ground-State Geometries. The ground-state geometries of carbazolenevinylene derivatives are the outcome of a tricky balance between steric and electronic (conjugation) effects. Table 1 lists some representative dihedral angles and bond lengths between the subunits of the compounds (Figure 1). In the case of PCP, it is expected that steric interactions between the vinylene hydrogen atoms and the adjacent H atoms in the ortho positions of the phenyl rings are weak and can be easily overcome by conjugation effects, which favor planarity. Therefore, a slightly nonplanar structure is found for PCP (see Table 1). The computed geometry is relatively close to those obtained from geometry optimizations of *trans*-stilbene at theoretical levels such as MM3,⁵¹ PM3,⁵² CASSCF,⁵³ and DFT/B3LYP,^{54,55} leading to nearly planar geometries. At such levels, the energy difference between these practically planar and fully planar structures is very small (of the order of 0.03–0.06 kcal mol⁻¹).

Table 1 shows that the ground-state geometry of TCT is slightly less twisted than its phenylene counterpart (PCP). Accordingly, the bond distance d_1 (see Figure 1) is shorter in TCT than in PCP. As expected, five-membered aromatic rings create less steric hindrance than six-membered rings. However, the electron-donating properties of the sulfur atoms should also play a role in the planarization of the thiophene derivatives.

The cyano-substituted carbazole derivatives are considerably more twisted, particularly near the cyano groups (θ_1), and their d_1 and d_2 bond distances are longer. This clearly indicates that the presence of cyano groups induces significant steric effects in the molecular frame. Similar theoretical results have been previously reported for several CN-PPVs.^{56,57}

3.2. Electronic Excitations and Correlation with the Absorption Spectra. The energy of the molecular orbitals has been calculated for all the derivatives. Since the first electronic transition of each compound involves the promotion of an

TABLE 2: HOMO and LUMO Energies and the HOMO–LUMO Energy Gap of Carbazolenevinylene Derivatives as Obtained from DFT/B3LYP/6-31G* Calculations

molecule	HOMO (eV)	LUMO (eV)	HOMO–LUMO (eV)
PCP	-4.994	-1.628	3.366
PCP-CN	-5.621	-2.434	3.187
TCT	-4.897	-1.738	3.159
TCT-CN	-5.518	-2.537	2.981

TABLE 3: Electronic Transition Data of $S_1 \leftarrow S_0$ for Carbazolenevinylene Derivatives as Obtained by TDDFT Calculations Performed on DFT/B3LYP/6-31G*-Optimized Geometries

molecule	energy (cm ⁻¹)	f^a	E_a (cm ⁻¹)
PCP	25119	2.12	25600
PCP-CN	23680	1.85	23600
TCT	23764	2.10	24500
TCT-CN	22237	1.89	22900

^a Oscillator strength of the $S_1 \leftarrow S_0$ electronic transition.

electron from the highest-occupied molecular orbital (HOMO) to the lowest-unoccupied molecular orbital (LUMO) (see below), only the energy of these orbitals has been compiled in Table 2. One can see that the replacement of phenyl groups by thiophene units slightly destabilizes the HOMO orbital and stabilizes the LUMO orbital. This shows that the LUMO orbital is more concentrated on the carbazole moiety and thus the HOMO–LUMO transition should possess some charge-transfer (CT) character. The overall effect is a decrease in the HOMO–LUMO energy gap of TCT compared to that of PCP. On the other hand, Table 2 shows that the incorporation of cyano groups in PCP and TCT derivatives stabilize both HOMO and LUMO orbitals, but LUMO orbitals show a larger decrease in energy. Consequently, a bathochromic shift is also expected for the HOMO–LUMO transition of cyano-substituted compounds compared to unsubstituted ones (see below).

Table 3 lists the energy and oscillator strength (f) for the $S_1 \leftarrow S_0$ electronic transition of the carbazolenevinylene derivatives. From these calculations, it is found that, for all the carbazole derivatives, the first electronic transition is dipole allowed and polarized along the long axis (x) of the molecules. Moreover, the lowest transition is in all cases dominated by a configuration in which an electron is excited from the HOMO to the LUMO. Similar theoretical results were obtained from TDDFT/B3LYP/6-31G* calculations performed on oligo(*p*-phenylenevinylene) (OPV).⁵⁸

For PCP, our theoretical calculations predict one intense electronic transition ($S_1 \leftarrow S_0$) at 25 119 cm⁻¹ (398 nm) with an oscillator strength of 2.12. The replacement of the phenylene rings by thiophene moieties induces a red shift in the $S_1 \leftarrow S_0$ electronic transition of TCT compared to that of PCP. According to the optimized geometries reported above, TCT is slightly less twisted than PCP in its ground electronic state (see Table 1). This effect should contribute to the $S_1 \leftarrow S_0$ bathochromic shift calculated for TCT. But to our opinion, the calculated shifts are too large to be attributed solely to these small conformational changes. Thus, as mentioned above, we believe that the electron donor properties of the thiophene rings induce some CT character to the HOMO–LUMO transition, giving rise to the red shift observed for the first electronic transition of TCT.

Table 3 shows that the singlet excitation energies for the cyano derivatives are significantly smaller than those obtained for the unsubstituted derivatives. Introduction of cyano groups in the vinylene moieties of PPV analogous compounds also lead

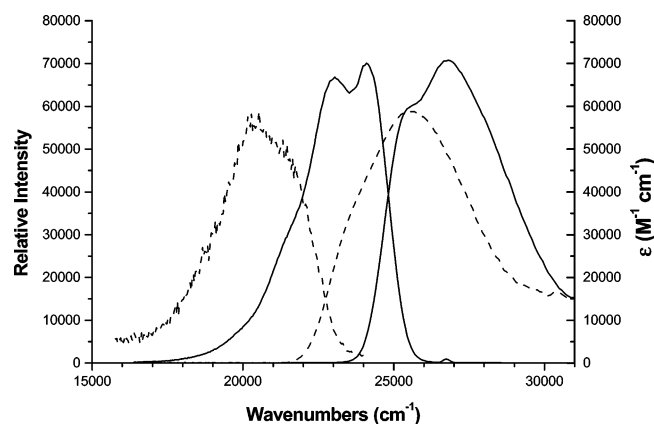


Figure 2. Absorption and fluorescence spectra of PCP (solid line) and PCP-CN (dashed line) in chloroform. The fluorescence intensities have been normalized relative to the absorption bands.

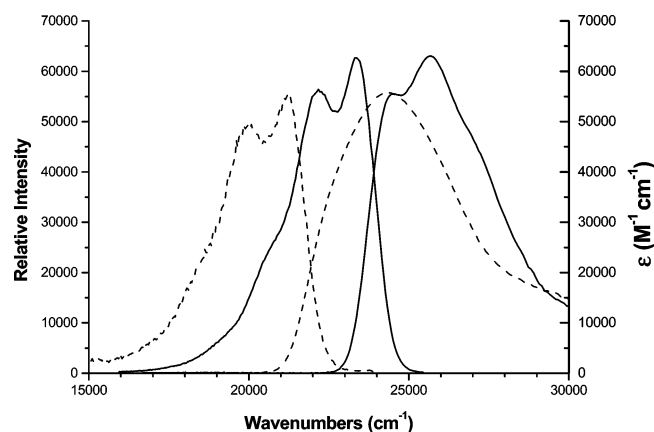


Figure 3. Absorption and fluorescence spectra of TCT (solid line) and TCT-CN (dashed line) in chloroform. The fluorescence intensities have been normalized relative to the absorption bands.

to a lowering of the $S_1 \leftarrow S_0$ excitation energy.^{59,60} Two effects might be responsible for this behavior: (1) an increase of the molecular planarity of these compounds and (2) a charge-transfer interaction due to the electron acceptor properties of the cyano groups. As mentioned above, PCP-CN is significantly more twisted than PCP in its ground state. This sole effect should induce a hypsochromic shift in the $S_1 \leftarrow S_0$ electronic transition of PCP-CN compared to that of PCP. Thus, the decrease of the excitation energy observed for the cyano-substituted compounds clearly shows the strong electron-withdrawing properties of the cyano groups, which more than cancel the blue shift caused by the steric effects and are responsible for the red shift observed. This goes along with the molecular orbital energies reported above, showing that the LUMO orbitals are more strongly stabilized than the HOMO orbitals by the presence of cyano groups. Finally, TCT-CN exhibits the smallest $S_1 \leftarrow S_0$ excitation energy, due to the combined effect of the electron-donor properties of the thiophene rings and the electron-acceptor properties of the cyano groups.

The absorption spectra of the 2,7-carbazolenevinylene-based conjugated compounds (the ethyl chains have been replaced by hexyl groups to achieve a better solubility) in dilute chloroform solution are shown in Figures 2 and 3. All spectroscopic data of the derivatives are listed in Table 4.

All compounds show a broad low-energy absorption band around 400–450 nm, typical of the $\pi-\pi^*$ transition of the conjugated PPV backbone.^{61–63} The first absorption band of PCP exhibits two vibronic bands at 25 600 and at 26 800 cm^{-1} , showing that this molecule possesses some rigidity in its ground

TABLE 4: Spectroscopic Parameters of 2,7-Carbazolenevinylenes in Chloroform at Room Temperature

molecule	ν_A^a (cm^{-1})	ϵ^b ($\text{M}^{-1} \text{cm}^{-1}$)	fwhm_A^c (cm^{-1})	ν_F^d (cm^{-1})	fwhm_F^e (cm^{-1})
PCP	25 600	69 700	4400	24 100	3100
PCP-CN	23 600	58 800	4700	21 300	3300
TCT	24 500	62 700	4200	23 400	2800
TCT-CN	22 900	55 700	4900	21 300	2900

^a Absorption wavenumbers taken at the maximum of the 0–0 vibronic peak. ^b Absorption coefficient at the maximum of the absorption band. ^c Full width at half-maximum (fwhm) of the absorption band. ^d Fluorescence wavenumbers at the maximum of the 0–0 vibronic peak. ^e Full width at half-maximum (fwhm) of the fluorescence band.

TABLE 5: Dihedral Angles and Bond Distances between Subunits of Carbazolenevinylene Derivatives in Their S_1 Electronic State as Obtained by RCIS/6-31G* Theoretical Calculations

molecules	dihedral angles (deg)		bond distances (\AA)		
	θ_1	θ_2	d_1	d_2	d_3
PCP	0.2	0.1	1.452	1.358	1.432
PCP-CN	26.8	7.9	1.475	1.370	1.429
TCT	0.26	0.34	1.437	1.361	1.430
TCT-CN	20.0	6.4	1.455	1.374	1.425

state. According to these experimental results, the optimized geometry of this molecule should not be much twisted, which agrees with the DFT results (see Table 1). The band located around 25 600 cm^{-1} (0,0 vibronic peak) is in good agreement with the $S_1 \leftarrow S_0$ electronic transition calculated at 25 119 cm^{-1} . It is worth pointing out that all theoretical calculations give the (0,0) transition energy equivalent to that in the gas phase. For this type of molecule, a bathochromic shift of about 1000–2000 cm^{-1} has to be assumed for the solvent shift. A good correlation is also obtained between the 0,0 absorption maximum and the computed $S_1 \leftarrow S_0$ transition energy of PCP-CN (see Table 3). Thus the significant bathochromic shift computed for the first electronic transition of PCP-CN is reproduced experimentally. Similarly, it was observed that the incorporation of cyano substituents in the vinylene moieties of phenylene vinylene compounds result in red shifts of their absorption and fluorescence spectra.^{64,65} Table 4 also shows that the absorption band of PCP-CN is wider than that of PCP and does not show any vibronic peaks. The lack of vibronic resolution would suggest the existence of torsional motions in the main chain, which probably originates from the addition of the bulky cyano group on the vinylene units, as has been previously reported for several CN-PPVs.^{56,57} This interpretation is in good agreement with the calculated geometry of PCP-CN reported in Table 1.

The replacement of the phenyl groups by thiophene rings provokes a red shift of the first absorption band in TCT. Moreover, the absorption spectrum of TCT exhibits a slightly better vibronic resolution and is slightly sharper than that of PCP (Table 4). This goes along with the better molecular planarity achieved for TCT. Finally, the energy of the first absorption band of TCT-CN is in good agreement with the computed $S_1 \leftarrow S_0$ electronic transition, confirming the important role played by the thiophene rings and the cyano groups in the decrease of the transition energy.

3.3. Geometry of the First Excited-State S_1 . Table 5 lists some representative geometrical parameters for the optimized S_1 geometries. For all four derivatives, d_1 and d_3 are significantly shortened, and d_2 significantly increases, compared to the respective bond lengths computed for the molecules in their

TABLE 6: Electronic Transition Energies ($E(S_1 \rightarrow S_0)$) of Carbazolenevinylene Derivatives as Obtained by TDDFT Performed on the RCIS/6-31G*-Optimized Geometries of S_1 Excited States

molecule	energy (cm ⁻¹)	f^a	E_f (cm ⁻¹)
PCP	22 914	2.33	24 100
PCP-CN	21 786	2.11	21 300
TCT	22 033	2.29	23 400
TCT-CN	20 610	2.10	21 300

^a Oscillator strength of the $S_1 \rightarrow S_0$ electronic transition.

TABLE 7: Photophysical Data for the Singlet States of 2,7-Carbazolenevinylenes in Chloroform at Room Temperature (298 K)

molecule	ϕ_F	τ_F (ns)	$10^{-8}k_F^a$ (s ⁻¹)	$10^{-8}k_{nr}^b$ (s ⁻¹)
PCP	0.91	1.54	5.9	0.58
PCP-CN	0.026	0.58	0.45	17
TCT	0.89	1.04	8.6	1.1
TCT-CN	0.058	0.56	1.0	17

^a $k_F = \phi_F/\tau_F$ (radiative fluorescence decay rate constant). ^b $k_{nr} = k_F(1 - \phi_F)/\phi_F$ (nonradiative fluorescence decay rate constant).

ground state (Table 1). In other words, the conjugation along the vinylene segments is enhanced in the S_1 state. It is therefore not surprising to observe that the overall geometry of each derivative is more planar in S_1 than in S_0 (see Tables 1 and 4). It is worth pointing out that PCP-CN and TCT-CN remain considerably twisted in the S_1 state, showing the very strong steric effects caused by the presence of cyano groups.

3.4. Emission Transition Energies and Correlation with the Fluorescence Spectra. From the optimized (relaxed) S_1 state geometries, the $S_1 \rightarrow S_0$ transition energies were calculated and the results are compiled in Table 6. For all the carbazole derivatives, it is observed that, after relaxation (optimization) of the S_1 excited state, the energy of the first electronic transition significantly decreases (see Tables 3 and 6). This transition should correspond to the emission energy of the derivatives. The absorption of a photon excites the molecules to the S_1 Franck–Condon state, which possesses the ground-state (S_0) geometry. After excitation, the molecules usually relax to their most stable geometry before the emission process occurs that leads to the FC region on the S_0 surface, which has the geometry of the relaxed S_1 state.

Figures 2–5 show the fluorescence spectra of the four compounds in dilute chloroform solution. Their spectral characteristics are reported in Table 4. One can see that the fluorescence peaks of the carbazole derivatives are in relatively good agreement with the computed emission energies (see Table 6). It is also observed that the fluorescence spectra of the four compounds are sharper and show a better-resolved vibronic structure compared to their respective absorption spectra (see Figures 2–5 and Table 3). These results give rise to the assumption of a more planar geometry of the molecules in their S_1 relaxed singlet state, an assumption that is in good agreement with the S_1 optimized geometries described above. However, the vibronic structure of the fluorescence spectrum of PCP-CN is very poor, which clearly shows that this carbazole derivative remains twisted in the relaxed S_1 state, as found from the theoretical calculations. It is worth pointing out that the fluorescence spectrum of this compound is very noisy since its fluorescence quantum yield is very low (see next section).

3.5. Molecular Photophysics. A summary of the photophysical parameters of the 2,7-carbazolenevinylenes in dilute chloroform solutions is given in Table 7, including fluorescence quantum yields (ϕ_F) and lifetimes (τ_F), and radiative (k_F) and

nonradiative (k_{nr}) decay constants for the lowest excited singlet state. The latter were calculated as ($k_F = \phi_F/\tau_F$) and ($k_{nr} = k_F(1 - \phi_F)/\phi_F$). In all cases, the fluorescence decays are well modeled by single-exponential functions, as shown by the usual statistical criteria of “goodness-of-fit” ($\chi^2 < 1.3$ and DW ≈ 1.7).

One can observe in Table 7 that PCP possesses a high ϕ_F value. The corresponding phenylenevinylene oligomer is also highly fluorescent with a quantum yield ϕ_F close to unity.^{32,66} This shows that the replacement of a phenyl ring by a carbazole moiety does not significantly affect the photophysical properties of this phenylenevinylene derivative. Table 7 also shows that the luminescence efficiency of TCT is rather similar to that of PCP ($\phi_F = 0.89$), but its τ_F value is shorter. This gives rise to higher k_F and k_{nr} values for TCT compared to the respective photophysical constants of PCP. The increase in k_{nr} observed for TCT is probably caused by the presence of heavy sulfur atoms. Indeed, for many oligothiophenes, it has been shown that the main deactivation pathway of the S_1 state involves a significant intersystem crossing process (k_{isc}) due to the presence of heavy sulfur atoms, which causes a decrease of their fluorescence quantum yields.^{67–69} On the other hand, the electron donor properties of the thiophene groups are probably responsible for the higher k_F value obtained for TCT.

The CN-containing derivatives exhibit much lower solution fluorescence quantum yields than their CN-free counterparts (see Table 7). A similar behavior has been reported for several CN-OPVs⁶⁶ and CN-PPVs^{56,70,71} and interpreted in terms of the noncoplanarity of the molecular backbones.^{56,66} Indeed, nonplanarity of the molecules enables torsional induced nonradiative deactivation by avoiding the planar quinoidal mesomeric structure in the S_1 state. In agreement with this statement, the nonradiative (k_{nr}) deactivation constants of the cyano derivatives are more than 1 order of magnitude higher than those of the unsubstituted compounds (see Table 7). This clearly shows the consequence of the twisted S_1 excited states on the nonradiative properties of these derivatives. However, internal CT interactions from the vinylene segments to the cyano groups could also contribute to the fluorescence quenching of the CN-substituted derivatives. Indeed, Jenekhe et al. have shown that strong intramolecular charge transfer in several donor/acceptor conjugated polymers is a major source of dramatic luminescence quenching in such materials.⁷²

It is worth pointing out that the incorporation of cyano groups on the vinylene moieties also induces an important decrease of the k_F values, which can also be related to the nonplanarity of the molecules in the S_1 state. The overlap of p_z orbitals is reduced in nonplanar conjugated systems, thus diminishing their radiative properties. Recently, similar photophysical results were reported for cyano-substituted phenylenevinylene derivatives.³² Since k_F is proportional to the oscillator strength (f) at the equilibrium geometry of S_1 , a decrease in these f values should be found for CN-substituted compounds. Indeed, one can see in Table 6 that a small reduction in f values for the S_1 -optimized geometries of PCP-CN and TCT-CN is calculated, but the magnitudes of the decrease obtained are much smaller than those expected from experimental k_F values.

Finally, Table 7 shows that the ϕ_F value of TCT-CN is about two times larger than that of PCP-CN, which is solely related to the k_F values of these compounds. These results could be explained by the slightly better planarity achieved by TCT-CN in the relaxed S_1 state, giving rise to a higher k_F value compared to that of PCP-CN.

4. Concluding Remarks

It is found that PCP and TCT almost reach planarity in their ground state (S_0). Replacement of the phenylene groups by thiophene moieties slightly decreases the torsional angle between the subunits. The incorporation of cyano groups in the 2,7-carbazolevinylene derivatives induces significant steric effects in the molecular frame. In the lowest excited state (S_1), all the molecules become more planar enhancing the conjugation along the vinylene segments. However, cyano derivatives remain considerably twisted in their S_1 electronic state.

For all four compounds, the first electronic transition is a strongly dipole allowed (large values of f) $\pi-\pi^*$ transition polarized along the long axis (x) of the molecule. The transition is dominated by the HOMO–LUMO excitation. In correspondence with the theoretical results, the absorption spectra of the investigated carbazole vinylene derivatives exhibit only one strong band in the visible region. The agreement between the calculated and experimental $S_1 \leftarrow S_0$ excitation energies was found to be excellent.

The relaxation (optimization) of the excited states induces a significant lowering of the first electronic transition of the carbazole derivatives. Emission transition energies are relatively well reproduced by TDDFT vertical transition energies computed from the S_1 -optimized geometries (RCIS/6-31G*). Moreover, as predicted from theoretical calculations, the overall shape of the absorption and fluorescence spectra indicates that the carbazole derivatives are more planar in their S_1 state.

The incorporation of cyano groups at the vinylene moieties induces red shifts in the absorption and fluorescence spectra of the carbazole derivatives, due to the electron-acceptor properties of the cyano groups. On the other hand, the addition of CN substituents causes a strong reduction of fluorescence yields. The low yields are mainly a consequence of nonplanarity caused by steric hindrance, which enables torsional induced nonradiative deactivation, giving rise to very high k_{nr} values. However, lower k_F values obtained for CN-substituted derivatives also play a role in the fluorescence quenching of these molecules.

The replacement of phenyl groups by thiophene moieties causes significant bathochromic shifts of the absorption and fluorescence bands, which are mainly due to the electron donor properties of the thiophene rings. Finally, it is observed that the fluorescence quantum yield of TCT is high and very similar to that of PCP. This is in sharp contrast with ϕ_F values of many oligothiophenes, which show smaller values of ϕ_F due to high intersystem crossing rate constants (k_{isc}) caused by the presence of heavy sulfur atoms.

Acknowledgment. This work was supported by NSERC strategic and research grants.

References and Notes

- (1) Dimitrakopoulos, C. D.; Malenfant, P. R. L. *Adv. Mater.* **2002**, *14*, 99.
- (2) Katz, H. E.; Bao, Z. *J. Phys. Chem. B* **2000**, *104*, 671.
- (3) Horowitz, G. *Adv. Mater.* **1998**, *10*, 365.
- (4) Brabec, C. J.; Sariciftci, N. S.; Hummelen, J. C. *Adv. Funct. Mater.* **2002**, *12*, 192.
- (5) Sariciftci, N. S.; Braun, D.; Zhang, C.; Srdanov, V. I.; Heeger, A. J.; Stucky, G.; Wudl, F. *Appl. Phys. Lett.* **1993**, *62*, 585.
- (6) Neher, D. *Macromol. Rapid Commun.* **2001**, *22*, 1365.
- (7) Leclerc, M. *J. Polym. Sci., Polym. Chem.* **2001**, *39*, 2867.
- (8) Mitschke, U.; Bauerle, P. *J. Mater. Chem.* **2000**, *10*, 1471.
- (9) Kraft, A.; Grimsdale, A. C.; Holmes, A. B. *Angew. Chem., Int. Ed.* **1998**, *37*, 402.
- (10) Burroughes, J. H.; Bradley, D. D. C.; Brown, A. R.; Marks, R. N.; MacKay, K.; Friend, R. H.; Burns, P. L.; Holmes, A. B. *Nature* **1990**, *347*, 539.

- (11) Belletête, M.; Bédard, M.; Bouchard, J.; Leclerc, M.; Durocher, G. *Can. J. Chem.* **2004**, *82*, 280.
- (12) Belletête, M.; Bédard, M.; Leclerc, M.; Durocher, G. *Synth. Met.* **2004**, *146*, 99.
- (13) Belletête, M.; Bédard, M.; Leclerc, M.; Durocher, G. *THEOCHEM* **2004**, *679*, 9.
- (14) Belletête, M.; Bouchard, J.; Leclerc, M.; Durocher, G. *Macromolecules* **2005**, *38*, 880.
- (15) Tirapattur, S.; Belletête, M.; Drolet, N.; Leclerc, M.; Durocher, G. *Chem. Phys. Lett.* **2003**, *370*, 799.
- (16) Bouchard, J.; Belletête, M.; Durocher, G.; Leclerc, M. *Macromolecules* **2003**, *36*, 4624.
- (17) Zotti, G.; Schiavon, G.; Zecchin, S.; Morin, J.-F.; Leclerc, M. *Macromolecules* **2002**, *35*, 2122.
- (18) Morin, J.-F.; Boudreault, P.-L.; Leclerc, M. *Macromol. Rapid Commun.* **2002**, *23*, 1032.
- (19) Morin, J.-F.; Leclerc, M. *Macromolecules* **2001**, *34*, 4680.
- (20) Morin, J.-F.; Leclerc, M. *Macromolecules* **2002**, *35*, 8413.
- (21) Morin, J.-F.; Beaupré, S.; Leclerc, M.; Lévesque, I.; D'Iorio, M. *Appl. Phys. Lett.* **2002**, *80*, 341.
- (22) Drolet, N.; Beaupré, S.; Morin, J.-F.; Tao, Y.; Leclerc, M. *J. Opt. A: Pure Appl. Opt.* **2002**, *4*, S252.
- (23) Roncali, J. *Chem. Rev.* **1997**, *97*, 173.
- (24) Burroughes, J. H.; Bradley, D. D. C.; Brown, A. R.; Marks, R. N.; Mackay, K.; Friend, R. H.; Burns, P. L.; Holmes, A. B. *Nature* **1990**, *347*, 539.
- (25) Friend, R. H.; Gymer, R. W.; Holmes, A. B.; Burroughes, J. H.; Marks, R. N.; Taliani, C.; Bradley, D. D. C.; Dos Santos, D. A.; Brédas, J. L.; Logdlund, M.; Salaneck, W. R. *Nature* **1999**, *397*, 121.
- (26) Jin, Y.; Ju, J.; Kim, J.; Lee, S.; Kim, J. Y.; Park, S. H.; Son, S.-M.; Jin, S.-H.; Lee, K.; Suh, H. *Macromolecules* **2003**, *36*, 6970.
- (27) Gillissen, S.; Jonforsen, M.; Kesters, E.; Johansson, T.; Theander, M.; Andersson, M. R.; Inganäs, O.; Lutsen, L.; Vanderzande, D. *Macromolecules* **2001**, *34*, 7294.
- (28) Mitschke, U.; Bäuerle, P. *J. Mater. Chem.* **2000**, *10*, 1471.
- (29) Detert, H.; Sugiono, E. *Synth. Met.* **2000**, *115*, 89.
- (30) Liu, M. S.; Jiang, X.; Liu, S.; Herguth, P.; Jen, A. K. Y. *Macromolecules* **2002**, *35*, 3532.
- (31) Pinto, M. R.; Hu, B.; Karasz, F. E.; Akcelrud, L. *Polymer* **2000**, *41*, 2603.
- (32) de Souza, M. M.; Rumbles, G.; Gould, I. R.; Amer, H.; Samuel, I. D. W.; Moratti, S. C.; Holmes, A. B. *Synth. Met.* **2000**, *111–112*, 539.
- (33) Morin, J.-F.; Drolet, N.; Tao, Y.; Leclerc, M. *Chem. Mater.* **2004**, *16*, 4619.
- (34) Hohenberg, P.; Kohn, W. *Phys. Rev.* **1964**, *136*, B864.
- (35) Kohn, W.; Sham, L. J. *Phys. Rev.* **1965**, *140*, A1133.
- (36) Frisch, M. J.; Trucks, G. W.; Schlegel, H. B.; Scuseria, G. E.; Robb, M. A.; Cheeseman, J. R.; Montgomery, J. A.; Vreven, T., Jr.; Kudin, K. N.; Burant, J. C.; Millam, J. M.; Iyengar, S. S.; Tomasi, J.; Barone, V.; Mennucci, B.; Cossi, M.; Scalmani, B.; Rega, G. N.; Petersson, G. A.; Nakatsuji, H.; Hada, M.; Ehara, M.; Toyota, K.; Fukuda, R.; Hasegawa, J.; Ishida, M.; Nakajima, T.; Honda, Y.; Kitao, O.; Nakai, H.; Klene, M.; Li, X.; Knox, J. E.; Hratchian, H. P.; Cross, J. B.; Adamo, C.; Jaramillo, J.; Gomperts, R.; Stratmann, R. E.; Yazyev, O.; Austin, A. J.; Cammi, R.; Pomelli, C.; Ochterski, J. W.; Ayala, P. Y.; Morokuma, K.; Voth, G. A.; Salvador, P.; Dannenberg, J. J.; Zakrzewski, V. G.; Dapprich, S.; Daniels, A. D.; Strain, M. C.; Farkas, O.; Malick, D. K.; Rabuck, A. D.; Raghavachari, K.; Foresman, J. B.; Ortiz, J. V.; Cui, Q.; Baboul, A. G.; Clifford, S.; Cioslowski, J.; Stefanov, B. B.; Liu, G.; Liashenko, A.; Piskorz, P.; Komaromi, I.; Martin, R. L.; Fox, D. J.; Keith, T.; Al-Laham, M. A.; Peng, C. Y.; Nanayakkara, A.; Challacombe, M.; Gill, P. M. W.; Johnson, B.; Chen, W.; Wong, M. W.; Gonzalez, C.; Pople, J. A. *Gaussian03*; Gaussian, Inc.: Pittsburgh, PA, 2003.
- (37) Becke, A. D. *J. Chem. Phys.* **1993**, *98*, 5648.
- (38) Lee, C.; Yang, W.; Parr, R. G. *Phys. Rev. B* **1988**, *37*, 785.
- (39) Ditchfield, R.; Hehre, W. J.; Pople, J. A. *J. Chem. Phys.* **1971**, *54*, 724.
- (40) Tretiak, S.; Mukamel, S. *Chem. Rev.* **2002**, *102*, 3171.
- (41) Casida, M. E. In *Recent Advances in Density Functional Methods, Part I*; Chong, D. P., Ed.; Singapore, World Scientific: 1995; p 155.
- (42) Gross, E.; Dobson, J.; Petersilka, M. *Top. Curr. Chem.* **1996**, *181*, 81.
- (43) Wilberg, K. B.; Stratmann, R. E.; Frisch, M. J. *Chem. Phys. Lett.* **1998**, *297*, 60.
- (44) Adamo, C.; Barone, V. *Chem. Phys. Lett.* **2000**, *330*, 152.
- (45) Bruel, R.; Amos, R. D.; Handy, N. C. *Chem. Phys. Lett.* **2002**, *355*, 8.
- (46) Yu, J. S. K.; Chen, W. C.; Yu, C. H. *J. Phys. Chem. A* **2003**, *107*, 4268.
- (47) Belletête, M.; Durocher, G.; Hamel, S.; Côté, M.; Wakim, S.; Leclerc, M. *J. Chem. Phys.* **2005**, *122*, 104303.
- (48) Foresman, J. B.; Head-Gordon, M.; Pople, J. A.; Frisch, M. J. *J. Phys. Chem.* **1992**, *96*, 135.

- (49) Eaton, D. F. *Pure Appl. Chem.* **1988**, *60*, 1107.
- (50) Zelent, B.; Ganguly, T.; Farmer, L.; Gravel, D.; Durocher, G. *J. Photochem. Photobiol.* **1991**, *56*, 165.
- (51) Kwasniewski, S. P.; François, J. P.; Deleuze, M. S. *J. Phys. Chem. A* **2003**, *107*, 5168.
- (52) Galvao, D. S.; Soos, Z. G.; Ramasesha, S.; Etemad, S. *J. Chem. Phys.* **1993**, *98*, 3016.
- (53) Molina, V.; Merchà, M.; Roos, B. O. *J. Phys. Chem. A* **1997**, *101*, 3478.
- (54) Kwasniewski, S. P.; Deleuze, M. S.; François, J. P. *Int. J. Quantum Chem.* **2000**, *80*, 672.
- (55) Choi, C. H.; Kertesz, M. *J. Phys. Chem. A* **1997**, *101*, 3823.
- (56) Egbe, D. A. M.; Kietzke, T.; Carbonnier, B.; Mühlbacher, D.; Hörhold, H.-H.; Neher, D.; Pakula, T. *Macromolecules* **2004**, *37*, 8863.
- (57) Chen, S.-A.; Chang, E.-C. *Macromolecules* **1998**, *31*, 4899.
- (58) Han, Y.-K.; Lee, S. U. *J. Chem. Phys.* **2004**, *121*, 609.
- (59) Cornil, J.; dos Santos, D. A.; Beljonne, D.; Brédas, J. L. *J. Phys. Chem.* **1995**, *99*, 5604.
- (60) Brédas, J. L. *Adv. Mater.* **1995**, *7*, 263.
- (61) Bao, Z.; Chen, Y.; Cai, R.; Yu, L. *Macromolecules* **1993**, *26*, 5281.
- (62) Vaidyanathan, S.; Dong, H.; Galvin, M. E. *Synth. Met.* **2004**, *142*, 1.
- (63) Brandon, K. L.; Bentley, P. G.; Bradley, D. D. C.; Dunmur, D. A. *Synth. Met.* **1997**, *91*, 305.
- (64) Döttinger, S. E.; Hohloch, M.; Hohnholz, D.; Segura, J. L.; Steinhuber, E.; Hanack, M. *Synth. Met.* **1997**, *84*, 267.
- (65) Döttinger, S. E.; Hohloch, M.; Segura, J. L.; Steinhuber, E.; Hanack, M.; Tompert, A.; Oelkrug, D. *Adv. Mater.* **1997**, *9*, 233.
- (66) Oelkrug, D.; Tompert, A.; Gierschner, J.; Egelhaaf, H.-J.; Hanack, M.; Hohloch, M.; Steinhuber, E. *J. Phys. Chem. B* **1998**, *102*, 1902.
- (67) Belletête, M.; Beaupré, S.; Bouchard, J.; Blondin, P.; Leclerc, M.; Durocher, G. *J. Phys. Chem. B* **2000**, *104*, 9118.
- (68) Becker, R. S.; Seixas De Malo, J.; Maçanita, A. L. Elisei, F. *Pure Appl. Chem.* **1995**, *87*, 9.
- (69) Rossi, R.; Ciofalo, M.; Carrita, A.; Ponterini, G. *J. Photochem. Photobiol., A* **1993**, *70*, 59.
- (70) Tillmann, H.; Hörbold, H.-H. *Synth. Met.* **1999**, *101*, 138.
- (71) Greenham, N. C.; Samuel, I. D. W.; Hayes, G. R.; Phillips, R. T.; Kessener, Y. A. R. R.; Moratti, S. C.; Holmes, A. B.; Friend, R. H. *Chem. Phys. Lett.* **1995**, *241*, 89.
- (72) Jenekhe, S. A.; Lu, L.; Alam, M. M. *Macromolecules* **2001**, *34*, 7315.